

Fatigue crack propagation behaviour of unidirectionally solidified γ/γ' - δ eutectic alloys

PHILIP E. BRETZ, RICHARD W. HERTZBERG

Department of Metallurgy and Materials Engineering, Lehigh University, Bethlehem, Pa 18015, USA

Fatigue crack propagation (FCP) studies were conducted on a series of γ/γ' - δ (Ni-Nb-Al) alloys by subjecting them to cyclic four-point bending loads at room temperature. The aluminium contents of the alloys investigated ranged from 1.5% to 2.5% by weight, with the niobium contents adjusted to maintain controlled eutectic microstructures. In addition to studies of as-grown alloys, heat treatments were performed on several of the alloys to determine the effect of resultant changes in microstructure on FCP behaviour. Crack growth rates from approximately 2×10^{-6} to 10^{-3} mm/cycle were recorded as a function of the crack tip stress intensity factor range. The growth rates for the heat-treated alloys differed little from the as-grown FCP behaviour. Comparison with other published results indicated that the addition of aluminium was beneficial to FCP resistance, although the level of aluminium addition (within the investigated range of 1.5 to 2.5% by weight) did not influence the crack growth rates. Based on a comparison with previously reported results, chromium additions were seen to have a detrimental effect on FCP behaviour. Fractographic studies revealed the superior fatigue behaviour of the γ/γ' - δ eutectic composite to be a result of repeated grain boundary delamination as the crack progressed through the microstructure.

1. Introduction

The development of *in situ* composite alloys holds considerable promise for future engineering applications. These composites are unique in that they can be manufactured directly from the melt by solidifying an eutectic or near-eutectic metal alloy under conditions of unidirectional heat flow. Because they combine the intrinsically superior mechanical properties of the "whisker-like" reinforcing phase with the dispersion strengthening advantages of a very fine spacing between the reinforcing elements, these alloys offer great potential for high strength. In addition, binary eutectic composites can frequently be further improved by ternary or higher order alloying.

The Ni-Ni₃Nb (γ - δ) system is one of the more attractive *in situ* composites. The advantages of directionally solidifying this binary eutectic were noted in several previous investigations [1-3]. Further improvements in mechanical

properties were achieved with the addition of Al, which led to the precipitation of Ni₃Al (γ') within the Ni matrix [4-6].

The fatigue properties of the γ - δ and γ/γ' - δ directionally solidified (DS) composites have been the subject of several research studies. The earliest work on the fatigue properties of γ - δ were reported by Hoover and Hertzberg [7]. Their room temperature S-N studies revealed this composite to have a notched round bar endurance limit 55% of the ultimate tensile strength in the longitudinal direction. A transition in the mechanisms of crack growth through the γ matrix from Stage I (propagation along active slip planes) to Stage II (striation formation) growth was noted. The authors concluded that the high cycle fatigue life of this DS composite was controlled by Stage I crack growth in the γ matrix.

The work of Mills and Hertzberg [8] was the first study of fatigue crack propagation (FCP)

behaviour in an eutectic composite. They found at room temperature that the crack growth behaviour of the γ - δ system obeyed the Paris relationship

$$\frac{da}{dn} = C\Delta K^m \quad (1)$$

where

$$\frac{da}{dn} = \text{incremental crack growth per cycle, mm/cycle}$$

$$\Delta K = \text{stress intensity factor range, MPa m}^{1/2}$$

$$C, m = \text{material constants: } 1 \times 10^{-11} \text{ (SI units) and 4.9 respectively.}$$

Heat treatment, which produced a Widmanstätten δ precipitate in the γ matrix, caused a moderate improvement in FCP behaviour. Some secondary cracking parallel to the fracture surface was noted in all specimens tested, and measured striation spacings were found to correlate well with macroscopic growth rate data.

Yuen and Leverant [9] examined the fatigue response of a Co-matrix composite reinforced with Cr_7C_3 (alloy 73C) and of $\gamma/\gamma'-\delta$ (0 and 6% Cr). They found crack growth rates in $\gamma/\gamma'-\delta$ to be far superior to the Co alloy. Comparison of their room temperature FCP results on $\gamma/\gamma'-\delta$ (6 Cr) with those of Mills and Hoover led them to conclude that γ' did not improve the fatigue behaviour of the alloy system. At 700 K, slightly lower crack growth rates were found in $\gamma/\gamma'-\delta$ without Cr than in the chromium-bearing $\gamma/\gamma'-\delta$. Yuen and Leverant also noted no influence of interlamellar spacing, λ , or of microstructural cellularity on the FCP behaviour. Some fatigue crack deflection by delamination was reported.

S-N studies of $\gamma/\gamma'-\delta$ (0 and 6 Cr) by Stoloff, *et al.* [10], yielded results which appear to differ with the findings of Yuen and Leverant. These authors reported a room temperature endurance limit for $\gamma/\gamma'-\delta$ of 84% of the UTS, whereas the Cr-bearing alloy had an endurance limit of only 58%. Their results suggested that the addition of Cr adversely affects the fatigue response of the $\gamma/\gamma'-\delta$ alloy. It should be noted that the tensile strengths of these alloys were very similar — 1193 MPa for 0 Cr as opposed to 1187 MPa for 6 Cr. Extensive delamination was found in the $\gamma/\gamma'-\delta$ (0 Cr), and the amount of faceting (Stage I crack growth) was less than in the $\gamma/\gamma'-\delta$ (6 Cr).

Consideration of the work of Yuen and Leverant and of Stoloff and co-workers raises several

questions. Other research in the $\gamma/\gamma'-\delta$ system has established that the addition of Al to the $\gamma-\delta$ system markedly increases the monotonic mechanical properties of the composite. For example, Gangloff and Hertzberg [3] determined an ultimate tensile strength of 745 MPa for $\gamma-\delta$ at room temperature, while Bertorello *et al.* [4], found an average tensile strength of 1165 MPa for $\gamma/\gamma'-\delta$ (2.5 wt% Al). One might then have expected the work of Yuen and Leverant to show an effect of Al addition on the fatigue behaviour of this alloy. This was not the case. Furthermore, the results of Stoloff *et al.* implied that Cr is detrimental to fatigue of the $\gamma/\gamma'-\delta$ alloy. Since the alloy studied by Yuen and Leverant was Cr-bearing, their data are inconclusive with regard to the effect of Al (i.e. γ') on the cyclic properties of this eutectic system.

Accordingly, a major objective of the present research will be to isolate the effect of varying Al content on the room temperature FCP and tensile properties of the $\gamma/\gamma'-\delta$ alloys. The influence of heat treatment on FCP behaviour of $\gamma/\gamma'-\delta$ will also be investigated. Finally, an attempt will be made to determine the role that delaminations play in controlling the FCP behaviour of the $\gamma/\gamma'-\delta$ eutectic alloys.

2. Experimental procedure

The alloys were prepared according to the procedure outlines in [11]. Directional solidification was accomplished with the aid of a high thermal gradient Bridgman apparatus similar to that described by Thompson and Lemkey [12]. All directional solidification was done at a speed of 10 cm h⁻¹ under a flowing He atmosphere. Heat treatments on selected as-grown pins were conducted in air. A solution treatment of 3 h at 1493 K was followed by oil quenching and subsequent ageing at 1223 ± 1 K in a diffusion-type furnace. FCP tests were run on specimens which had been aged for 357 h.

TABLE I Etching techniques

Modified Marble's reagent (MMR)	Etchant for twinning (ET)	Electropolishing (EP)
4 g $\text{Cu}_2\text{SO}_4 \cdot 5\text{H}_2\text{O}$	35 ml HNO_3	37 ml H_3PO_4
60 ml ethanol	2 ml HF	56 ml glycerin
20 ml HCl	63 ml H_2O	7 ml H_2O
20 ml H_2O		
Swab for 5 sec	Immerse for 25 sec	12 V d.c. 1.0–1.2 A cm ⁻²

Metallographic specimens were prepared by conventional mechanical polishing, followed by one of the three etching techniques listed in Table I. Metallographic examinations were conducted using a Zeiss Axiomat optical microscope and an ETEC Autoscan scanning electron microscope.

Tensile properties of each alloy were measured on an Instron testing machine at a cross-head speed of 0.51 mm min^{-1} . The nominal size of the threaded-end tensile bars was 4 mm gauge diameter \times 20 mm gauge length. A 13 mm strain gauge extensometer was used to determine accurately the yield point of each alloy.

Cyclic testing was performed on an MTS closed-loop electro-hydraulic system under tension-tension conditions at frequencies of 20 or 40 Hz and with a stress ratio of $R \leq 0.1$ ($R = \sigma_{\text{min}}/\sigma_{\text{max}}$). Crack growth was monitored by a travelling microscope with a calibrated vernier dial. A four-point bending fixture previously described by Mills and Hertzberg [8] was used in this investigation. The specimen size for the FCP tests was 114 mm \times 12 mm \times 2.5 mm, with steel tabs being bonded to the ends of the specimen to ensure lateral stability. For these tests, the major and minor spans of the fixture were 102 and 76 mm, respectively. A starter notch 2 mm deep was cut into the centre of the tensile side of each specimen by an electro-discharge machining apparatus. To produce the longitudinal fracture surface profiles, smaller specimens were cut from the previously tested bars, pre-notched, and then fatigue-cracked to some arbitrary length.

The crack growth rate data were analysed on a CDC 6400 computer with the growth rate at a

TABLE II Alloy compositions

Alloy	wt % Ni	wt % Nb	wt % Al
$\gamma/\gamma'-\delta$ (1.5 Al)	76.5	22.0	1.5
(1.9 Al)	76	22.1	1.9
(2.5 Al)	76	21.5	2.5

(Percentages are calculated from weights of raw materials in the master heat.)

measured crack length a_i being calculated from the following formula

$$\left(\frac{da}{dn}\right)_i = \frac{a_{i+1} - a_{i-1}}{n_{i+1} - n_{i-1}} \quad (2)$$

Because of the relatively large plastic zone size to crack length ratio, it was necessary to include a plasticity correction in the data reduction programme. The details of this iterative correction are given in [11].

Examination of the fracture surfaces was carried out using both scanning electron (SEM) and transmission electron (TEM) microscopic techniques. For SEM studies, the surfaces were lightly coated with an evaporated carbon film to ensure a stable signal and examined in an ETEC Autoscan SEM operated at a 20 kV accelerating potential. Standard two-stage platinum-carbon replicas were prepared for TEM examination. An RCA EMU-3G electron microscope operated at 50 and 100 kV and a Philips EM 300 electron microscope operated at 60 kV were used for this phase of the study.

Examination of the fracture surface profile was accomplished by mounting, polishing, and etching (ET etchant) fatigue-cracked but unbroken

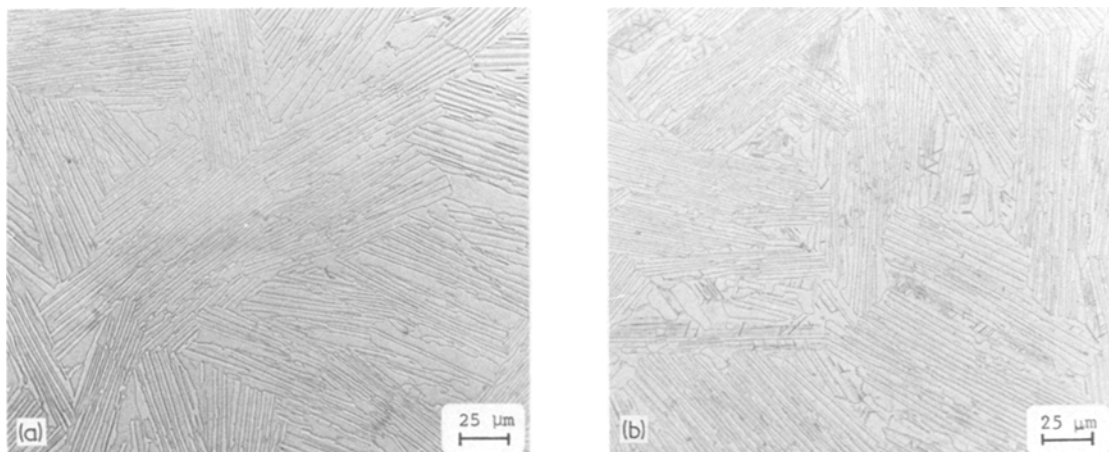


Figure 1 Optical photomicrographs of $\gamma/\gamma'-\delta$ (1.5 Al). Preparation - MMR. (a) As-grown (b) heat-treated.

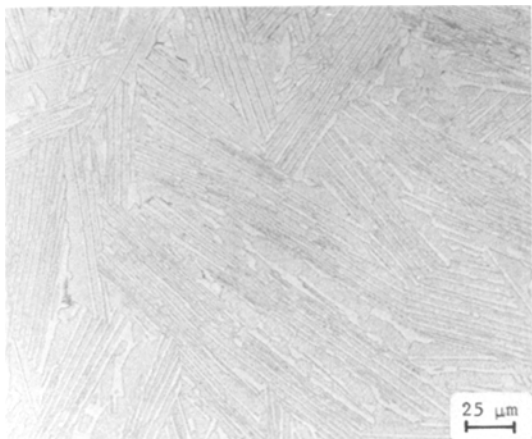


Figure 2 Optical photomicrograph of $\gamma/\gamma'-\delta$ (2.5 Al). Preparation – MMR.

samples. In this manner, mating fracture surfaces could be examined directly. A Zeiss Axiomat optical microscope was employed for these examinations.

3. Presentation and discussion of results

3.1. Microstructures

The compositions of the three alloys tested are given in Table II and the microstructures shown in the first two illustrations. The fully lamellar structure of the as-grown 1.5 Al alloy can be seen in Fig. 1a with Widmanstätten δ precipitates as a result of heat treatment shown in Fig. 1b. The structures of the 1.9 Al alloys were similar to the 1.5 Al material, although found to be slightly δ -rich. Fig. 2 shows some cellularity in the otherwise lamellar microstructure of the 2.5 Al $\gamma/\gamma'-\delta$ alloy.

The range of γ' precipitate size observed in as-grown microstructures containing 1.5 to 2.5 Al can be seen in Fig. 3. The average γ' size was 0.1 to 0.2 μm in diameter as could be seen in the alloy containing 2.5 Al. Smaller γ' could also be seen in the high Al content material. The large γ' eutectic grain boundary film in the 2.5 Al alloy was not visible in the alloy containing 1.5 Al.

TABLE III Yield strength

Alloy	σ_{YS} (0.2% offset) (MPa)
$\gamma/\gamma'-\delta$ (1.5 Al) as-grown	1100
(1.5 Al) heat-treated	1041
(1.9 Al) as-grown	1020
(1.9 Al) heat-treated	1034
(2.5 Al) as-grown	1052

3.2. Tensile tests

The effects of Al content and heat treatment on the room temperature yield strength of the $\gamma/\gamma'-\delta$ alloys are presented in Table III. It can be seen that neither the variation in Al nor the heat treatment (357 h at 1223 K) had a significant effect on the yield strength. These data suggest that the strength of $\gamma/\gamma'-\delta$ was optimized by the small γ' precipitates in the 1.5 Al alloy, and that increasing the Al content to 2.5% did not further enhance the strength of the alloy.

3.3. Fatigue crack propagation behaviour

The results of the FCP tests are presented in Figs. 4 to 8 in the form of log crack growth rate (da/dn) versus log stress intensity factor range (ΔK) plots. The least-squares line for the as-grown 1.5 Al (Fig. 4) is plotted on the other four sets of data to provide a comparison among the alloys. The Paris constants for this line were $C = 8 \times 10^{-12}$ (SI units)

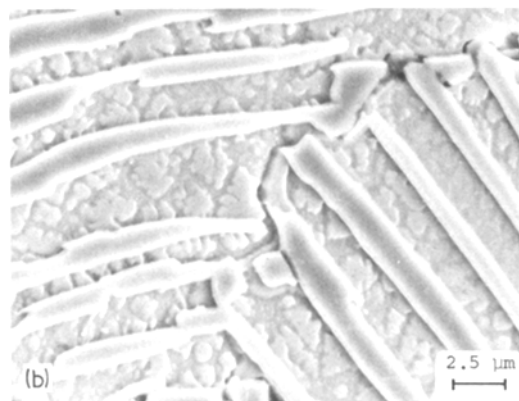
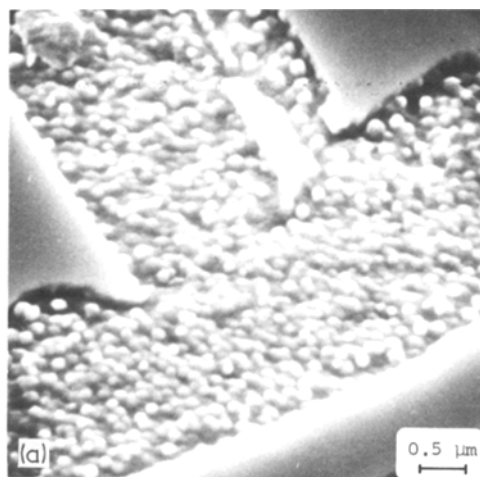


Figure 3 SEM photomicrograph showing γ' size variation. Preparation – EP. (a) 1.5 Al, (b) 2.5 Al.

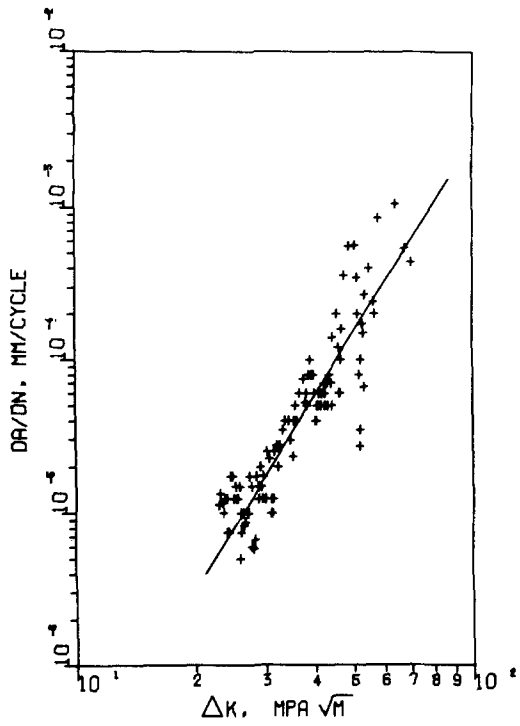


Figure 4 Crack growth rate versus stress intensity range for 1.5 Al (as-grown).

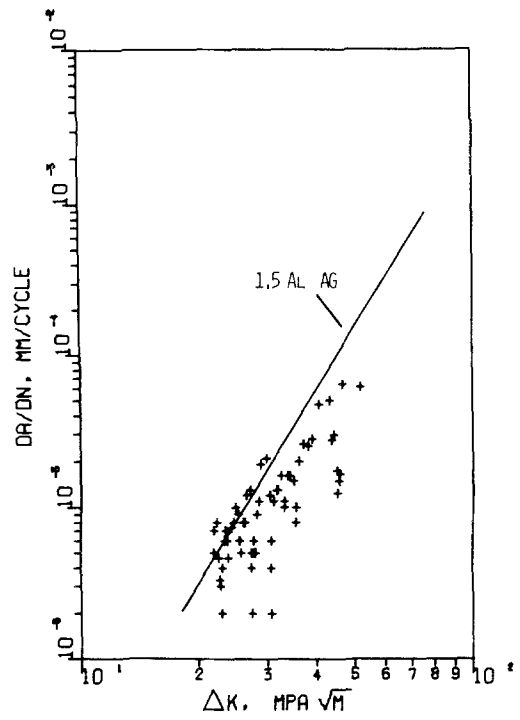


Figure 6 Crack growth rate versus stress intensity range for 1.9 Al (as-grown).

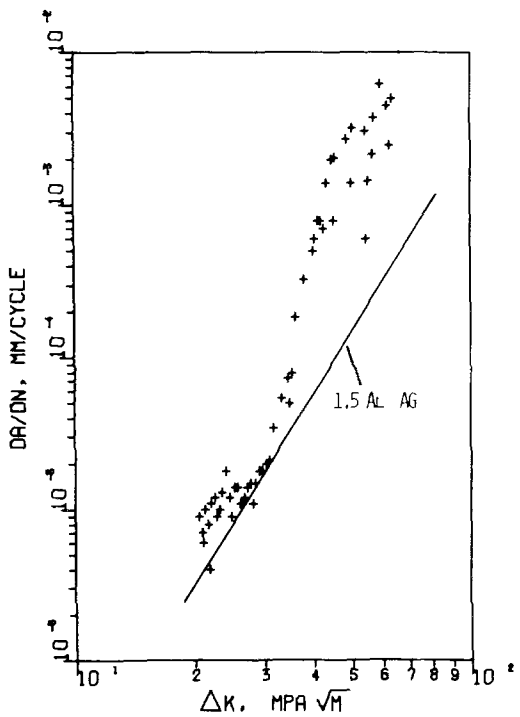


Figure 5 Crack growth rate versus stress intensity range for 1.5 Al (heat-treated).

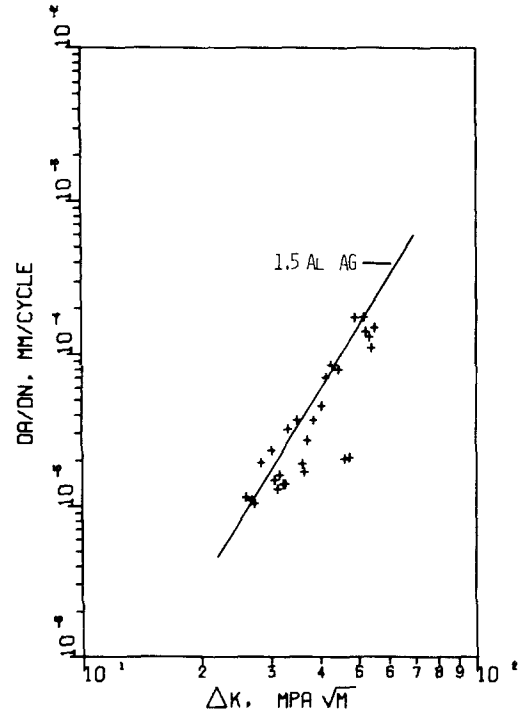


Figure 7 Crack growth rate versus stress intensity range for 1.9 Al (heat-treated).

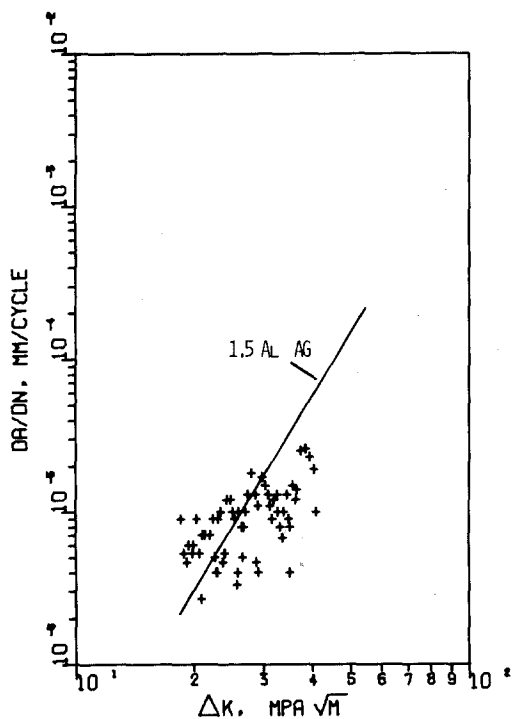


Figure 8 Crack growth rate versus stress intensity range for 2.5 Al (as-grown).

and $m = 4.28$. The slope is somewhat lower than that found by Mills and Hertzberg for the γ - δ system ($m = 4.9$). The rather limited range of data for several of the alloys resulted from the tendency of these samples to delaminate and split longitudinally early in the test.

Several important observations can be made from these results. The first is that a variation in the Al content of the as-grown alloys did not significantly affect the crack growth rate behaviour of γ/γ' - δ eutectic composites. A second observation is that the heat treatments of the 1.5 and 1.9 Al composites had a mixed effect on crack growth rates. Note that the data for the heat-treated and as-grown 1.9 Al alloy lie on the least-squares line for the as-grown 1.5 Al. By contrast, growth rates for heat-treated 1.5 Al alloy were somewhat higher than for the as-grown condition, especially at higher ΔK levels.

Comparison of the present results with the work of Mills and Hertzberg [8] indicates that the addition of Al to the binary γ - δ DS eutectic dramatically improved the FCP behaviour of the alloy. Fig. 9 shows γ/γ' - δ (0 Cr) to exhibit crack growth rates at a given ΔK level that are an order

of magnitude lower than those for the γ - δ alloy. We suggest that this difference in FCP response may be rationalized on the basis of stacking fault energy (SFE) considerations. In the high SFE nickel matrix of the γ - δ system, there will be a considerable propensity for cross-slip. The addition of Al to this system will reduce the SFE of the matrix and precipitate the coherent γ' phase in the matrix, both of which will reduce the tendency for matrix cross-slip. Studies by McEvily and Boettner [13] and Miller [14] have similarly shown that a reduction in SFE will decrease crack growth rates. McEvily and Boettner theorized that the beneficial effect of lower SFE was due to the increased difficulty of cross-slip. Following a parallel line of reasoning, Miller postulated that decreasing the SFE interfered with the formation of the dislocation substructure which is a precursor to fracture. Therefore, the reduced propensity for cross-slip in the matrix of the γ/γ' - δ eutectics as a result of the lower matrix SFE and the presence of the coherent γ' precipitate is considered to be a reason for the lower crack growth rates in these alloys relative to the γ - δ fatigue behaviour.

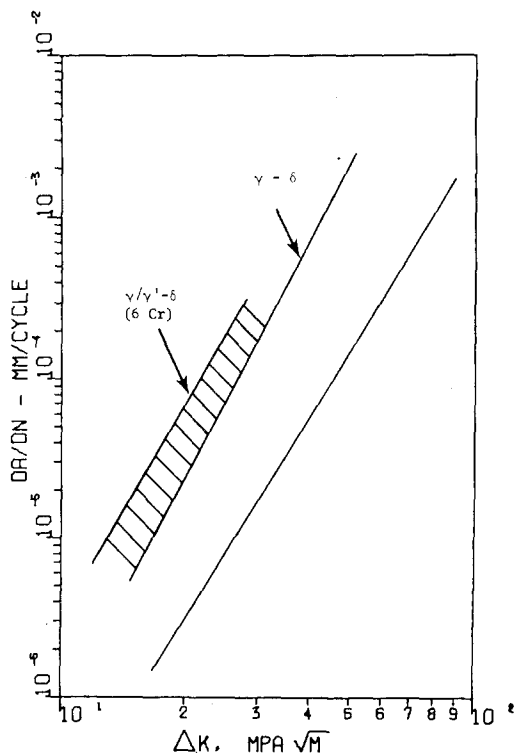


Figure 9 Comparison of present work with FCP data on γ - δ and γ/γ' - δ (6 Cr).

A similar improvement in fatigue response was reported by Kim *et al.* [15] in the $\text{Ag}_3\text{Mg}-\text{AgMg}$ eutectic composite. These authors noted improved fatigue resistance when this alloy was heat treated to produce long-range order in the matrix. The transition from wavy to planar glide upon ordering was suggested as an explanation for the observed improvement in resistance to fatigue damage.

The data shown in Fig. 9 suggest that the addition of Cr must have had a detrimental effect on the FCP behaviour of $\gamma/\gamma'-\delta$ alloy. The room temperature growth rates reported by Yuen and Leverant [9] were at least one order of magnitude higher than for the $\gamma/\gamma'-\delta$ eutectic without Cr. As was mentioned in the Introduction, Yuen and Leverant did find somewhat lower growth rates in the 0 Cr over the 6 Cr alloy at 700 K, although no comparison was made at room temperature. Since these authors did report equivalent fatigue behaviour in these two alloys at 1200 K, their results might indicate a divergence in the FCP behaviour of the alloys as test temperature was decreased. If so, then a marked difference in crack growth rates at room temperature would seem reasonable. However, no attempt was made in this study to determine the role that Cr plays in the fatigue behaviour of the $\gamma/\gamma'-\delta$ system.

3.4. Fractography

Scanning electron microscopy provided a direct comparison between the present study of $\gamma/\gamma'-\delta$ and the results of Mills and Hertzberg for the $\gamma-\delta$ system. It was found that the fatigue fracture surfaces of all $\gamma/\gamma'-\delta$ alloys tested were significantly rougher than the $\gamma-\delta$ alloy. Fig. 10 illustrates the dramatic difference between $\gamma-\delta$ and a typical example of the $\gamma/\gamma'-\delta$ alloys. The rough surfaces of the $\gamma/\gamma'-\delta$ alloys appeared to be the result of extensive delamination which produced many large vertical steps on the fracture surfaces.

To confirm that extensive delamination was occurring in the $\gamma/\gamma'-\delta$ alloys, longitudinal fracture surface profiles were prepared by mounting and polishing mating halves of cracked but unbroken fatigue specimens.

Examination of these samples revealed that extensive delamination and crack bifurcation had occurred in all alloys tested. Fig. 11 shows a typical fracture profile where the erratic path of the crack is evident. It was found that approximately 90% of the delaminations were intergranu-

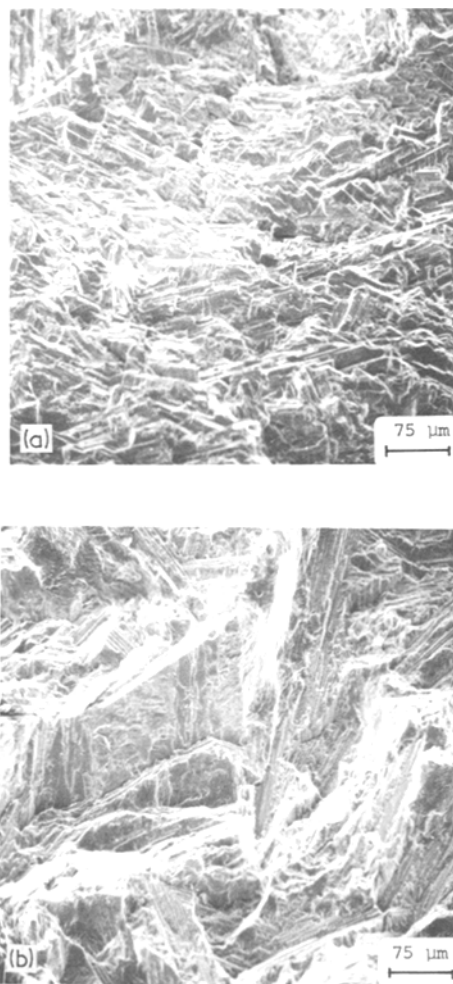


Figure 10 SEM fractographs comparing typical surface features of $\gamma-\delta$ and $\gamma/\gamma'-\delta$. (a) $\gamma-\delta$ (as-grown), (b) $\gamma/\gamma'-\delta$ (1.9 Al, as-grown).

lar; i.e., at the eutectic colony boundaries instead of along lamellar interfaces. The character of the delaminations was found to be independent of aluminium content and specimen heat treatment.

The predominance of intergranular delamination was significant in light of the variation in grain boundary morphology among the alloys. Whereas the eutectic containing 2.5 Al had an extensive γ' eutectic grain boundary film of significant size, the 1.5 Al alloy had no visible γ' film (Fig. 3). Apparently, the tendency toward delamination in these alloys was not controlled by the presence of a large γ' film.

Because of the delamination and resultant crack blunting, the crack is forced to reinitiate continuously. Hence, the average crack growth is expected



Figure 11 Typical longitudinal fracture surface profile illustrating erratic crack growth and delaminations. Preparation – ET.

to be lower with increasing amounts of delamination. In related fashion, the repeated delamination of the crack is believed to be responsible for the large amount of scatter in the FCP data (Figs. 4 to 8); the data showed repeated slowing of the macroscopic growth rates, frequently in conjunction with the appearance of a delamination on the surface of the specimen during the test. As was previously mentioned, the paucity of data for several of the alloys was due to the tendency for these metals to delaminate and split longitudinally, thereby prematurely terminating normal transverse crack growth. The beneficial influence of delaminations in slowing macroscopic growth rates in $\gamma/\gamma'-\delta$, evident from the present work, closely parallels recently reported fatigue results of other metals in which delaminations were found to be beneficial [15, 17–19].

Transmission electron microscopy of the replicated fracture surfaces revealed surface features similar to those seen by Mills and Hertzberg. The smooth, featureless fracture of the δ platelets and the Stage I faceting of the γ matrix were both evident in all $\gamma/\gamma'-\delta$ alloys (Fig. 12).

The Stage I–II transition seen in the $\gamma-\delta$ system was not observed in the present work, with the extent of faceted growth being greater in the $\gamma/\gamma'-\delta$ alloys than in the $\gamma-\delta$. This observation is consistent with the fact that the addition of Al lowers the SFE of the Ni matrix, thereby increasing the propensity for crystallographic fracture. In contrast, no clear evidence for fatigue striations was found on the $\gamma/\gamma'-\delta$ fracture surfaces examined in this investigations.

3.5. Summary remarks on experimental results

The results of these FCP tests on the $\gamma/\gamma'-\delta$ system indicated that the addition of Al to the base $\gamma-\delta$ alloy acted to reduce fatigue crack growth rates. Additionally, the fractographic studies suggested that the tendency for these composites to delaminate enhanced their FCP behaviour. The following question might then reasonably be asked: Did the addition of Al to $\gamma-\delta$ increase the propensity for the alloy to delaminate?

Because of the predominance of grain boundary delamination, one might reasonably be tempted to look for a brittle grain boundary film as an explanation. As was previously discussed, however, the large γ' grain boundary film seen in the 2.5 Al alloy was not visible in the composite containing only

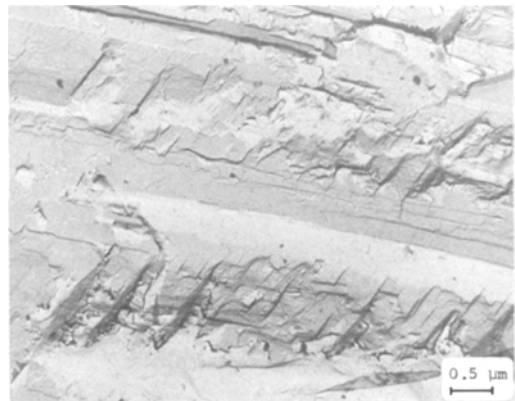


Figure 12 TEM fractograph showing smooth fracture of δ platelets and faceted (Stage I) crack growth in the γ matrix.

1.5 wt% Al. An interesting trend in the FCP data did suggest some influence of this large γ' film, nonetheless. The available range of data was greatest for the 1.5 Al alloys and least for the 2.5 Al composition. Premature terminal delamination was previously cited as the reason for the minimal range of data for the high Al eutectic. The premature termination of crack growth by delamination occurred earliest in the composition which contained the large, continuous γ' film at the eutectic colony boundaries. Therefore, although the size of the γ' film did not appear to influence the macroscopic growth rates, the size did have an effect on the extent of stable fatigue crack growth prior to failure.

A qualitative explanation for the beneficial effect of Al on the fatigue behaviour of the $(\gamma-\delta)/(\gamma/\gamma'-\delta)$ system may be found instead in a "weakest link" argument. In the $\gamma-\delta$ system, it is postulated that the γ matrix is weak enough (in a relative sense) so as to allow for the passage of a crack. Consequently, delaminations would be more infrequent because of the ease of transgranular propagation. However, the addition of Al is seen to strengthen the γ matrix by precipitation of γ' : the hardness of the as grown composites increases from DPH 323 for $\gamma-\delta$ [20] to 440 for $\gamma/\gamma'-\delta$ (1.5 Al). The γ/γ' matrix would then be expected to more effectively resist crack propagation, so that when the crack would reach a eutectic colony boundary, the path of least resistance would be along the boundary rather than through the adjacent grain. Hence, grain boundaries in $\gamma/\gamma'-\delta$ could become the weakest part of the composite structure as a result of the addition of Al to the alloy.

4. Conclusions

(1) Improved FCP behaviour resulted from the addition of Al to $\gamma-\delta$ to produce the $\gamma/\gamma'-\delta$ eutectic composite. In the investigated range of Al addition (1.5 to 2.5 wt%), there was no difference in the effect of Al content on crack growth rates. The enhanced FCP resistance of the $\gamma/\gamma'-\delta$ composite was related to the inhibition of cross-slip brought about by the addition of aluminium to the $\gamma-\delta$ binary.

(2) The superior fatigue response of the $\gamma/\gamma'-\delta$ composites was also a result of repeated delaminations at the crack tip. These delaminations blunted the crack and required reinitiation of the fatigue crack for continued growth.

(3) Delamination in the $\gamma/\gamma'-\delta$ alloys was predominantly intergranular in nature, with only 10% of observed delaminations being interlamellar.

(4) A comparison of the present work with that of Yuen and Leverant on the $\gamma/\gamma'-\delta$ (6 Cr) system indicated that the addition of Cr was detrimental to the FCP behaviour of the composite.

(5) The yield strength of a $\gamma/\gamma'-\delta$ eutectic composite was not sensitive to Al content in the range of 1.5 to 2.5 wt% Al.

Acknowledgements

The authors wish to express their sincere appreciation to INCO Limited, whose fellowship provided financial support for this research programme. The financial assistance of the National Aeronautics and Space Administration under Grant NGR 39-007-007 and the technical assistance of the Bethlehem Steel Corporation are also gratefully acknowledged.

References

1. R.T. QUINN, R.W. KRAFT and R.W. HERTZBERG, *Trans. ASM* **62** (1969) 38.
2. W. R. HOOVER and R. W. HERTZBERG, *Met. Trans.* **2** (1971) 1283.
3. R. P. GANGLOFF and R. W. HERTZBERG, Proceedings of the Conference on In Situ Composites, Lakeville, Conn. (1972) p.83.
4. H. R. BERTORELLO, R. W. HERTZBERG and R. W. KRAFT, Proceedings of the 2nd Conference on In Situ Composites, Bolton Landing, NY (1976) p. 517.
5. X. NGUYEN-DINH, M. S. Thesis, Lehigh University, (1977).
6. F. D. LEMKEY and E. R. THOMPSON, Proceedings of the Conference on In Situ Composites, Lakeville, Conn. (1972) p. 105.
7. W. R. HOOVER and R. W. HERTZBERG, *Met. Trans.* **2** (1971) 1289.
8. W. J. MILLS and R. W. HERTZBERG, "Fatigue of Composite Materials", ASTM STP 569 (American Society for Testing and Materials, Metals Park, Ohio, 1975) p. 5.
9. A. YUEN and G. R. LEVERANT, *Met. Trans.* **7A** (1976) 1443.
10. N.S. STOLOFF, W.A. JOHNSON, J.E. GROSSMAN, and C. KOBURGER, Technical Report No. 2 on Contract N00014-75-C-0503, NR031-745, Rensselaer Polytechnic Institute, Troy, NY (1976).
11. P. E. BRETZ, M. S. Thesis, Lehigh University (1977).
12. E. R. THOMPSON and F. D. LEMKEY, *Composite Mater.* **4** (1974) 101.
13. A. J. McEVILY, Jr. and R. C. BOETTNER, *Acta Met.* **11** (1963) 725.
14. G. A. MILLER, Sc. D. Dissertation, Massachusetts Institute of Technology (1965).

15. Y. G. KIM, G. E. MAURER and N. S. STOLOFF, "Fatigue of Composite Materials, ASTM STP 569 (American Society for Testing and Materials, Metals Park, Ohio, 1975) p. 210.
16. P. C. J. GALLAGHER, *Met. Trans.* **1** (1970) 2429.
17. A. W. THOMPSON, J. C. WILLIAMS, J. D. FRANSEN and J. C. CHESNUTT, Proceedings of the 3rd International Titanium Conference, Moscow (1976).
18. G. J. MAY, *Met. Trans.* **6A** (1975) 1115.
19. R. B. SCARLIN, *ibid.* **7A** (1976) 1535.
20. H. R. BERTORELLO, R. W. HERTZBERG, W. MILLS, R. W. KRAFT and M. NOTIS, *Acta Met.* **24** (1976) 271.

Received 31 January and accepted 6 July 1978.